

102683-10-3; Ik (CC entry), 102696-49-1; Ik (boric acid entry), 102683-11-4; II (CC entry), 102696-50-4; II (boric acid entry), 102683-12-5; 2-isopropoxy-1,3,2-benzodioxaborole, 61676-63-9; 4-(methylamino)-3-penten-2-one, 14092-14-9; 4-(ethylamino)-3-penten-2-one, 50967-59-4; 4-(isopropylamino)-3-penten-2-one, 59487-11-5; 4-(butylamino)-3-penten-2-one, 57717-00-7; 4-(propylamino)-3-penten-2-one, 83696-44-0; 2-(butylamino)-1-propenyl phenyl ketone, 76943-80-1; 2-(methylamino)-2-phenylethenyl phenyl ketone, 891-16-7; 2-(ethylamino)-2-phenylethenyl phenyl ketone, 20964-96-9; 2-(propylamino)-2-

phenylethenyl phenyl ketone, 57167-94-9; 2-(isopropylamino)-2-phenylethenyl phenyl ketone, 102683-00-1; 2-(butylamino)-2-phenylethenyl phenyl ketone, 57167-95-0; 2-(methylamino)-2-phenylethenyl 4-chlorophenyl ketone, 102683-01-2.

Supplementary Material Available: Listings of fractional coordinates, anisotropic and isotropic temperature factors, and bond lengths and bond angles (3 pages). Ordering information is given on any current masthead page.

Contribution from the Department of Chemistry,
Rutgers, The State University of New Jersey, New Brunswick, New Jersey 08903

Organotin Intercalation Compounds of FeOCl: Synthesis, ^{57}Fe and $^{119\text{m}}\text{Sn}$ Mössbauer and Infrared Spectroscopy, and Powder X-ray Diffraction Studies

J. E. Phillips[†] and R. H. Herber*

Received January 2, 1986

Four new organotin intercalates of FeOCl were synthesized and studied by infrared and variable-temperature ^{57}Fe and $^{119\text{m}}\text{Sn}$ Mössbauer spectroscopies and by X-ray powder diffraction. These systems were chosen to provide a detailed microscopic spectroscopic examination of both the host and the guest species as well as a comprehensive picture of the guest-host interaction. The neat organotins, 4-(CH_3)₃Sn($\text{C}_5\text{H}_4\text{N}$) (P1), (CH_3)₃SnN(CH_3)₂ (A1), (CH_3)₂Sn[$\text{N}(\text{CH}_3$)₂]₂ (A2), and Sn[$\text{N}(\text{CH}_3$)₂]₄ (A4), all show evidence for an increase in tin coordination upon intercalation to form nominally FeOCl(P1)_{1/7.5} (INP1), FeOCl(A1)_{1/5.5} (INA1), FeOCl(A2)_{1/8} (INA2), and FeOCl(A4)_{1/16} (INA4). The intercalation process is described as a redox process where an electron is first donated to the FeOCl lattice with the corresponding formation of a pyridinium ligand for INP1 and an iminium ligand for INA1, INA2, and INA4, which then enter between the layers of the FeOCl matrix. The intercalated species in INP1 is described as an associated moiety with both four- and five-coordinate tin and an abnormally low charge transfer to the lattice, which is attributed to the large size of the guest. Data for INA1, INA2, and INA4 are interpreted in terms of six-coordinate tin species in which the fifth and sixth sites are lattice chlorines. An additional organic intercalation compound, FeOCl-[(CH_3)₂N⁺=CH₂]_{1/5}[Cl⁻]_{1/10}, was also prepared and studied as a model compound for the intercalation of the organotin amines. ^{57}Fe Mössbauer relaxation calculations have been used to determine the extent of the charge transfer to the lattice.

Introduction

Iron oxychloride is a strongly anisotropic compound that can admit guest molecules between its layers to form a variety of intercalation compounds. The detailed structure of FeOCl was reported by Lind,¹ confirming the earlier work of Goldsztaub.² The unit cell parameters are $a = 378.0$, $b = 791.7$, and $c = 330.2$ pm. The orthorhombic space group is P_{mmm} . The structure consists of a corrugated (in two dimensions) iron-oxygen framework sandwiched between planes of chlorine atoms to form one layer of the lamellar material. The interlayer bonding is a weak van der Waals interaction. In the intercalation process these weak interactions are broken (except for the intercalates formed with unsolvated alkali cations) and the layers are pried apart to accommodate the guest species. When the limiting stoichiometry is reached, the resulting FeOCl intercalation compounds consist of alternating guest and host layers with each van der Waals layer expanded to its final dimension.

A number of organic, organometallic, and metallic species have been intercalated into FeOCl, including pyridine and substituted pyridines,³ ammonia⁴ and amines,⁵ phosphines and phosphites,⁶ alkali metals,⁷ and metallocenes.⁸ Although few guest structural or orientation studies have been carried out on FeOCl-containing systems, several important conclusions have been reached for the related ammonia and pyridine intercalates of TaS₂, as well as for isostructural host materials such as NbS₂ and TiS₂. Guest species that can be intercalated into FeOCl usually also form intercalation compounds in TaS₂. A plot of the interlayer expansion in FeOCl vs. the analogous parameter in TaS₂ was shown to have a strong linear correlation,⁹ suggesting that the guest orientation and guest-host bonding interaction in the two hosts are similar. This allows the more comprehensive TaS₂ structural studies to be generalized to the corresponding FeOCl intercalates.

A widely accepted redox mechanism for intercalation into these matrices was proposed by Schöllhorn.¹⁰ An electron is first donated to the lattice from a potential guest species, presumably near the surface of the lattice. This is followed by intercalation of a positively charged species, either the original product of the redox process or a more stable positively charged species formed by further reaction. A number of intercalation compounds of FeOCl and TaS₂ are formed under mild conditions, indicating that the metal host atoms in these lattices are easily reduced. In almost all cases, neutral guest species or solvents are co-intercalated and are usually thought of as solvating species for the charged guest moieties.

Previous studies in this laboratory^{3,9,11,12} have used X-ray powder diffraction, ^{57}Fe Mössbauer spectroscopy, and Fourier transform infrared spectroscopy to study organic intercalates of FeOCl. In the present study a number of organotin compounds, which can participate in the Schöllhorn mechanism, have been synthesized and successfully intercalated into FeOCl. Employing organotins as guest species permits the additional use of $^{119\text{m}}\text{Sn}$ Mössbauer spectroscopy to elucidate the changes in the guest as well as the host moieties and serves as an additional probe of the intercalated layer system. The present study summarizes the results of both

- (1) Lind, M. D. *Acta Crystallogr., Sect. B: Struct. Crystallogr. Cryst. Chem.* **1970**, *B26*, 1058.
- (2) Goldsztaub, S. C. R. *Hebd. Seances Acad. Sci.* **1934**, *198*, 667.
- (3) Herber, R. H.; Maeda, Y. *Inorg. Chem.* **1981**, *20*, 1409.
- (4) Hagenmuller, P.; Portier, J.; Barbe, B.; Bouclier, P. Z. *Anorg. Allg. Chem.* **1967**, *355*, 209.
- (5) Weiss, A.; Sick, E. Z. *Naturforsch., B: Anorg. Chem., Org. Chem.* **1978**, *B33*, 1087.
- (6) Herber, R. H.; Maeda, Y. *Inorg. Chem.* **1980**, *19*, 3411.
- (7) Palvadeau, P.; Coic, L.; Rouxel, J. *Mater. Res. Bull.* **1978**, *13*, 221.
- (8) Halbert, T. R.; Scanlon, J. C. *Mater. Res. Bull.* **1979**, *14*, 415.
- (9) Eckert, H. E.; Herber, R. H. *J. Chem. Phys.* **1984**, *80*, 4526.
- (10) Schöllhorn, R.; Zagefka, H. D.; Butz, T.; Lerf, A. *Mater. Res. Bull.* **1979**, *14*, 369.
- (11) Herber, R. H.; Cassell, R. A. *J. Chem. Phys.* **1981**, *75*, 4669.
- (12) Salmon, A.; Eckert, H.; Herber, R. H. *J. Chem. Phys.* **1984**, *81*, 5206. Herber, R.; Salmon, A. *Hyperfine Interact.*, in press.

[†] Present address: Engelhard Corp., East Newark, NJ 07029.

Table I. X-ray Powder Diffraction Data for FeOCl and the Five Intercalates of FeOCl

	FeOCl ^a	INP1	INA1	INA2	INA4	INIM ^b
stoichiometry		1/7.5	1/5.5	1/8	1/16	
lattice params						
<i>a</i> , pm	378.0	380.0	381.2	381.4	380.8	378.9
<i>b</i> , pm	791.7	2823.3	2277.2	2309.4	2311.8	2389.9
<i>c</i> , pm	330.2	331.3	331.2	332.8	333.2	330.9
interlayer expansion, pm		620.0	346.9	363.0	364.2	403.3
guest area available, 10 ⁵ pm ²		4.72	3.47	5.08	10.15	
proposed species area, 10 ⁵ pm ²		(2×) 4.58	4.22	4.95	7.36	

^a Reference 1. ^b FeOCl[(CH₃)₂N⁺=CH₂]_{1/5}[Cl⁻]_{1/10}.

⁵⁷Fe and ¹¹⁹Sn Mössbauer studies of a number of organotin intercalates of FeOCl.

Experimental Section

Starting Materials. FeOCl was prepared from anhydrous FeCl₃ and Fe₂O₃ by using a vapor-transport technique⁶ and from FeCl₃·6H₂O by using a thermal decomposition process.¹³

Due to the moisture and oxygen sensitivity of the starting materials and the compounds synthesized in this work, all manipulations were carried out under an inert atmosphere (argon or nitrogen) and under rigorously anhydrous conditions. Tetrahydrofuran and hexane were dried by refluxing with lithium aluminum hydride and distilled. Ethanol was dried over magnesium ethoxide and benzene was dried over sodium wire before they were distilled. The intercalated compounds were characterized by elemental analysis by Robertson Laboratory Inc., Florham Park, NJ. The purity of known organotin compounds was determined by NMR spectroscopy with a Varian T-60 spectrometer.

The syntheses of 4-(trimethylstannyl)pyridine (P1) and 4-(trimethylstannyl)pyridine-trimethylstannyl chloride (P2) have been described in an earlier study.¹⁴ The syntheses of (CH₃)₃SnN(CH₃)₂ (A1), (CH₃)₂Sn[N(CH₃)₂]₂ (A2), and [(CH₃)₂N]₄Sn (A4) were carried out by using the method of Jones and Lappert.¹⁵ In this procedure lithium dimethylamide is reacted with the appropriate organotin chloride or tin tetrachloride. Repeated attempts of the synthesis of A2 by adding a dimethyltin dichloride solution to a slurry of lithium dimethylamide were unsuccessful, but the compound was successfully synthesized by slowly adding the slurry to the organotin solution. After being stirred for 2 h at room temperature, the reaction mixture was flash evaporated, removing both the solvents and product and leaving a small amount of solid residue. If the reaction mixture is distilled without this separation, the product converts to a syrupy mass. The solvents were distilled off, and the product was distilled at reduced pressure.

Syntheses of the Intercalation Compounds. All of the intercalates were synthesized by using either vapor transport FeOCl, which had been ground and then sieved through a 200-mesh screen, or the unground solid obtained by the thermal decomposition process. Previous studies¹² are in agreement with the present results that there are no significant differences in the properties of intercalation compounds which differ only in the method of FeOCl preparation. The FeOCl was placed in a glass ampule and evacuated overnight on a vacuum line to a pressure of 10⁻⁵ Torr. The ampules were occasionally heated to 100 °C to aid in the removal of volatiles. The organotin was added (by cold trapping if possible) in addition to a solvent as noted. The mixtures were then freeze-thawed three times and finally sealed under vacuum.

Synthesis of FeOCl(P1)_{1/7.5} (INP1). This compound was synthesized by soaking FeOCl with excess neat organotin for 10 months at 50 °C, although much shorter reaction periods also resulted in products showing comparable elemental analysis data. After the reaction period was complete, the sample was rinsed with dry hexane and dried. Anal. Calcd for FeOCl(P1)_{1/7.5}: C, 9.18; H, 1.25; Cl, 25.40; N, 1.34. Found: C, 9.03; H, 1.47; Cl, 24.40; N, 1.31.

Synthesis of FeOCl(A1)_{1/5.5} (INA1). A mixture of 1.5 g of A1, 1.5 g of FeOCl, and 40 mL of hexane was allowed to react for 2 months at room temperature. The product was then rinsed with dry hexane. Anal. Calcd for FeOCl(A1)_{1/5.5}: C, 7.53; H, 1.89; Cl, 24.43; N, 1.76. Found: C, 7.16; H, 1.96; Cl, 24.05; N, 1.80.

Synthesis of FeOCl(A2)_{1/8} (INA2). A mixture of 1.5 g of A2, 1.5 g of FeOCl, and 40 mL of hexane was allowed to react for 7 weeks at 50

°C. The ampule was opened and the solid filtered off and rinsed with dry hexane. Anal. Calcd for FeOCl(A2)_{1/8}: C, 6.58; H, 1.66; Cl, 25.89; N, 2.56. Found: C, 6.18; H, 1.71; Cl, 25.89; N, 2.63.

Synthesis of FeOCl(A4)_{1/16} (INA4). This compound was intercalated neat (excess) into 1.5 g of FeOCl for 3 weeks at 50 °C, and the product was then rinsed with ether. Anal. Calcd for FeOCl(A4)_{1/16}: C, 4.78; H, 1.20; Cl, 28.20; N, 2.78. Found: C, 4.74; H, 1.50; Cl, 27.82; N, 2.73.

Synthesis of FeOCl[(CH₃)₂N⁺=CH₂]_{1/5}[Cl⁻]_{1/10} (INIM). Dimethylmethyleammonium chloride, (CH₃)₂N⁺=CH₂Cl⁻, (0.11 g) was added to 0.50 g of FeOCl and 3 mL of hexane. The sample was allowed to react for 3 weeks at 50 °C and then rinsed with chloroform. Anal. Calcd for FeOCl[(CH₃)₂N⁺=CH₂]_{1/5}[Cl⁻]_{1/10}: C, 5.88; H, 1.32; Cl, 31.84; N, 2.29. Found: C, 5.69; H, 1.38; Cl, 33.43; N, 2.09.

The Mössbauer data were obtained on microcrystalline powders by using a constant-acceleration spectrometer described elsewhere.⁶ The ⁵⁷Fe Mössbauer samples were placed between high-purity aluminum foils and then sandwiched between copper cell holders. The ¹¹⁹Sn Mössbauer intercalation samples were mounted similarly by using a 2-mm spacer to provide approximately 3 mm of sample thickness, due to the low abundance of Sn in the sample. In the latter spectral studies, a 0.025-mm-thick palladium foil was mounted on the detector side of the cell holder to remove X-rays originating from the tin atoms of the sample. The liquid organotin sample cell consisted of a copper plate with a 15-mm-diameter hole drilled in the center. Thin glass disks were then mounted on each face with epoxy to provide an airtight enclosure. A suitable thickness Teflon spacer was used between the glass plates to reduce the optical thickness of the sample. The sample was introduced into the cell with a syringe through a tapped hole perpendicular to the face of the cell. The cell was then sealed with a screw fitted with a Teflon washer.

Spectrometer calibration was effected by using the magnetic hyperfine spectrum of metallic iron at room temperature. The iron isomer shifts are reported with respect to the centroid of this spectrum. The tin isomer shifts are reported with respect to an absorber spectrum of barium stannate at room temperature. Data reduction was carried out on the Rutgers IBM 370/178 computer using a least-squares matrix-inversion Lorentzian fitting routine in which line position, line width, and resonance effect magnitude are allowed to vary as free parameters. Where noted, the line widths were restricted to obtain fits to overlapping resonances. Temperature control over the time period required for data acquisition at a given temperature (typically 4–24 h) was better than ±0.5 °C.

The infrared data were obtained with an IBM IR/32 Fourier transform infrared spectrometer. The infrared pellets were prepared by using ~0.5 wt % samples in KBr. Liquid samples were observed in commercial liquid cells.

The samples for powder X-ray diffraction were ground and placed in 0.3-mm capillaries, which were then mounted in a 114.6-mm-diameter Debye-Scherrer camera.

Results and Discussion

X-ray Powder Diffraction. The X-ray film data for FeOCl and the five intercalation compounds are included in the supplemental data. The observed unit cell parameters are summarized in Table I along with the area available for the guest species (i.e. the interlamellar area per guest molecule) as calculated from the stoichiometry. In the case of INP1, the presence of strong lines due to unintercalated FeOCl makes the stoichiometry somewhat uncertain. A cobalt X-ray source was used because of the substantial fluorescence encountered when a copper anode was used. The interlayer *b* axis of FeOCl is observed to double and expand upon intercalation, as has been noted previously in the case of all non-alkali-metal intercalation compounds of FeOCl.⁴ The doubling of the *b* axis is due to the shifting of every other host layer to form larger vacancies to accommodate the guest species. The data also show a substantial number of X-ray lines for the or-

(13) Stuve, J. M.; Ferrante, M. J.; Richardson, D. W.; Brown, R. R. *Rep. Invest.—U. S., Bur. Mines* **1980**, R.I. 8420; *Chem. Abstr.* **1980**, 93, 10260.

(14) Phillips, J. E.; Herber, R. H. *J. Organomet. Chem.* **1984**, 268, 39.

(15) Jones, K.; Lappert, M. F. *J. Chem. Soc.* **1965**, 1944.

(16) Herber, R. H.; Eckert, H. *Phys. Rev. B: Condens. Matter* **1985**, 31, 34.

Table II. Symmetry Elements and Systematic Absences for the FeOCl Structures Discussed in the Text

sym element	structure			
	D	A	B	C
2-fold screw along				
<i>a</i>	Y	Y	Y	Y
<i>b</i>	N	Y	Y	Y
<i>c</i>	Y	Y	Y	Y
glide planes				
<i>b</i> /2	$\perp a$	N	Y	N
<i>c</i> /2	$\perp a$	N	N	N
<i>b</i> /2 + <i>c</i> /2	$\perp a$	N	N	Y
<i>a</i> /2	$\perp b$	N	N	N
<i>c</i> /2	$\perp b$	N	Y	N
<i>a</i> /2 + <i>c</i> /2	$\perp b$	Y	Y	Y
<i>a</i> /2	$\perp c$	N	N	N
<i>b</i> /2	$\perp c$	N	N	Y
<i>a</i> /2 + <i>b</i> /2	$\perp c$	N	N	Y

Absences^a

structure A: $0kl, k$ odd; $h0l, l$ odd; $h0l, h + l$ odd
 structure B: $0kl, k + l$ odd; $hk0, h + k$ odd; $h0l, h + l$ odd
 structure C: $hk0, h$ odd; $h0l, h$ odd; $h0l, h + l$ odd
 structure D: $h0l, h + l$ odd; $h00, h$ odd; $00l, l$ odd

^aStructures A–C also have $h00, h$ odd; $0k0, k$ odd; and $00l, l$ odd.

ganotin intercalates, which could not be assigned by using the given unit cell parameters. These lines are thought to be supercell reflections, observed as a consequence of the orderly arrangement of the guest organotin species. A simple calculation of the expected total X-ray intensity (proportional to Z^2 times the atomic density) of the guest species relative to that originating from the host shows that the guest intensity should be from 19% to 51% of that of the host for the observed stoichiometries. Attempts were made to fit the unassigned reflections to supercells generated from small integer multiples of the unit cell parameters. Since these were unsuccessful, it is concluded that the arrangement of the tin atoms in the lattice is not a simple one. The arrangements are expected to be well ordered because of the substantial intensities observed for the unassigned lines.

The strongest X-ray reflections for the organic intercalates of FeOCl are usually the (020), (130), and (200) lines. The (130) reflections in the four organotin intercalates are all very strong. Curiously, this reflection is not observed in INIM. Conversely, the (120) reflection is missing in the organotins but is very strong in INIM. Because these observations might be accounted for by structural differences, the possible structures consistent with a doubling of the *b* axis parameter were examined in more detail to determine if the resulting systematic absences could account for the observed and unobserved reflections. The layer packing structures consistent with a doubled *b* axis parameter are a shift of every other FeOCl layer by *a*/2, by *a*/2 and *c*/2, and by *c*/2. The three possibilities are designated A, B, and C, respectively, and, along with FeOCl itself (structure D), are shown in Figure 1. The symmetry elements and systematic absences associated with these four structures are shown in Table II.

The X-ray data for INIM are only consistent with structure A, and the data for INA4 are only consistent with structure B. The remaining organotin intercalate data have X-ray assignments that are consistent with both structures A and B. Structures A and C form vacancies that resemble tunnels. Structure B has vacancies that are roughly spherical cavities.

The interlayer expansion of INP1 over FeOCl is 620 pm, significantly larger than the value of 535 pm reported³ for FeOCl(py)_{1/4}, where py is pyridine. The long axis of P1 in the intercalate is concluded to be in the *ac* plane since the observed interlayer expansion is too small for other orientations differing only slightly from this. The orientation of the pyridine C2 axis was shown by neutron diffraction to be parallel to the layers in perdeuterated TaS₂(py)_{1/2}¹⁷ and NbS₂(py)_{1/2}.¹⁸ For this orien-

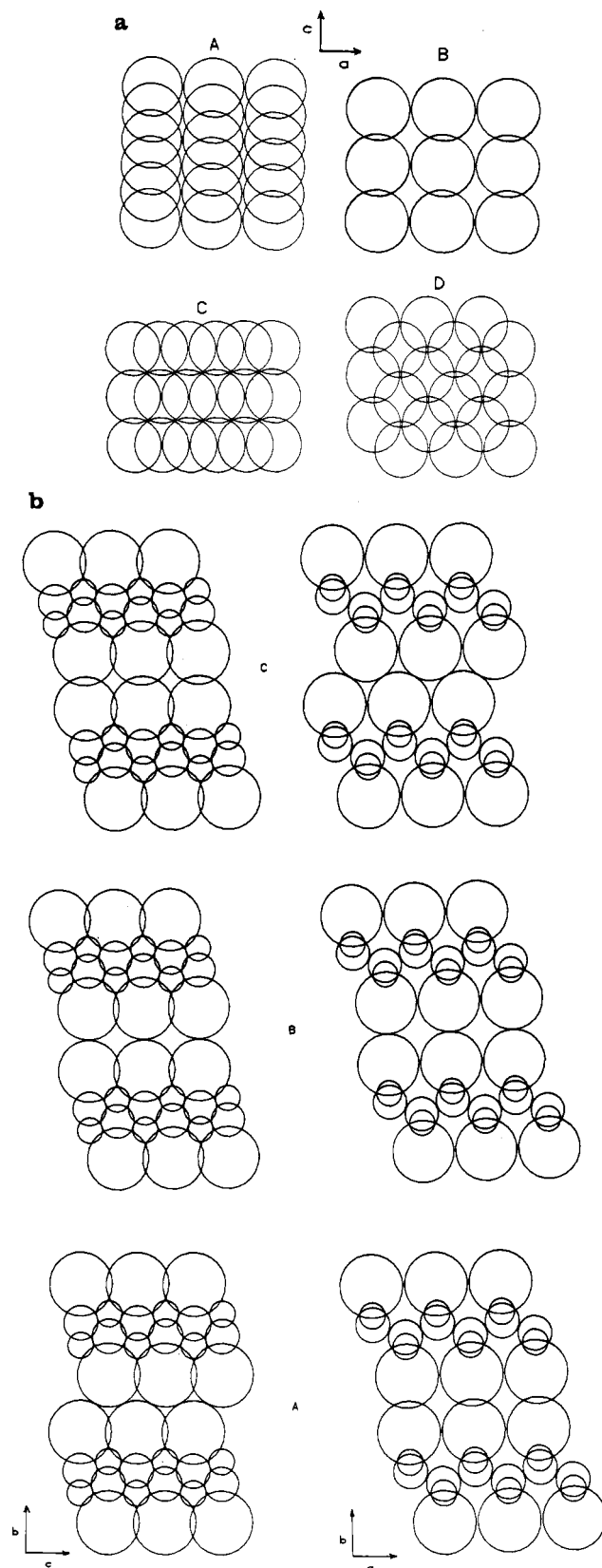


Figure 1. FeOCl layer packing arrangements discussed in the text: (a) view parallel to the *b* axis; (b) views perpendicular to the *b* axis.

tation in FeOCl(py)_{1/4} the calculated covalent dimension of pyridine along the interlayer axis is 513 pm, in reasonable agreement with the observed value. Neither the pyridine nor the tetrahedral trimethylstannyl group in INP1 is quite large enough

(17) Riekel, C.; Fischer, C. O. *J. Solid State Chem.* 1979, 29, 181.

(18) Riekel, C.; Hohlwein, D.; Schöllhorn, R. *J. Chem. Soc. Chem. Commun.* 1976, 863.

Table III. ^{57}Fe Mössbauer Parameters for the Organotin Intercalation Compounds

	INP1	INA1	INA2	INA4
Fe(III)				
IS(78 K), mm s^{-1}	0.480 (9)	0.500 (17)	0.500 (11)	0.492 (24)
QS(78 K), mm s^{-1}	1.036 (19)	1.104 (16)	1.136 (11)	1.113 (40)
IS(298 K), mm s^{-1}	0.394 (10)	0.446 (18)	0.424 (28)	0.422 (46)
QS(298 K), mm s^{-1}	0.807 (27)	0.714 (28)	0.810 (21)	0.742 (35)
$-\text{d}(\ln A)/\text{d}T \times 10^3$	2.264	2.415	1.685	2.211
Fe(II)				
IS(78 K), mm s^{-1}	1.220 ^a	1.201	1.193	1.229
QS(78 K), mm s^{-1}	2.424 ^a	2.461	2.521	2.586
charge transfer (% of Fe)	6.1	10.25	10.25	11.0

^a 100 K spectrum. The 78 K spectrum was partially magnetically ordered.

to account for the interlayer expansion. The actual moiety responsible for holding the host layers apart can be postulated, *vide infra*, on the basis of $^{119}\text{m}\text{Sn}$ Mössbauer spectroscopy. The orientation of the pyridine ring in INP1 may be the same as in the pyridine intercalates since it may be inferred that the repulsion between the chlorine lone pairs and the π -electron density of the pyridine ring favors this geometry.

In contrast to INP1, the organotin amine intercalates have considerably smaller interlayer expansions of 346.9–364.2 pm. Unless a tin–ligand bond has been broken, the only reasonable explanation is that the four tin ligand bonds flatten to a *quasi*-planar array. All three organotin amine intercalates are consistent with structure B—in which the chlorines on either side of the van der Waals gap are eclipsed. It is proposed that the guest species in these compounds are present as six-coordinate species, with two matrix chlorine atoms occupying the fifth and sixth coordination sites. The tin–chlorine bond length of ~ 310 pm is intermediate between the stronger (240 pm) and weaker associated (354 pm) tin–chlorine bonds in dimethyltin dichloride.¹⁹ Dimethyltin dichloride has a distorted octahedral chain structure with equivalent, asymmetrically bridged chlorines.

The calculated area of the hypothetical planar neat organotins is compared with the available area calculated from the stoichiometry and is included in Table I. The results show that the stoichiometries for INP1 and INA2 correspond well with a “full” monolayer of guest species between each layer of FeOCl. The results for INA4 indicate that the intralayer packing arrangement of the guest species has a considerable amount of open space. The density of the INA1 guest species in the guest layer is considerably more than expected from the molecular dimensions of the guest.

^{57}Fe Mössbauer Spectroscopy. The four organotin intercalation compounds were also studied by variable-temperature ^{57}Fe Mössbauer spectroscopy. A summary of the results is presented in Table III and typical 78 and 298 K ^{57}Fe Mössbauer spectra are shown in Figure 2. The spectra consist of a quadrupole split doublet, with the isomer shift and quadrupole splitting consistent with high-spin Fe(III). The 78 K spectrum exhibits an additional resonant absorption, which was identified in an earlier study¹¹ of FeOCl intercalation compounds as one member of a quadrupole split doublet, the missing component lying beneath the more negative velocity majority peak. The resulting isomer shift and quadrupole splitting of the minority doublet correspond to high-spin Fe(II). The appearance of an Fe(II) resonance is a consequence of the redox mechanism for the intercalation process.

The Mössbauer spectra of the organic intercalates of FeOCl have been treated^{9,16} quantitatively in terms of a relaxation process. In this model the electrons donated to the lattice are not localized on individual iron atoms but can “hop” to nearby iron sites, the rate of hopping being a function of temperature. At liquid-nitrogen temperature the hopping rate is slow compared to the Mössbauer time scale ($\sim 10^{-7}$ s), and individual Fe(III) and Fe(II) contri-

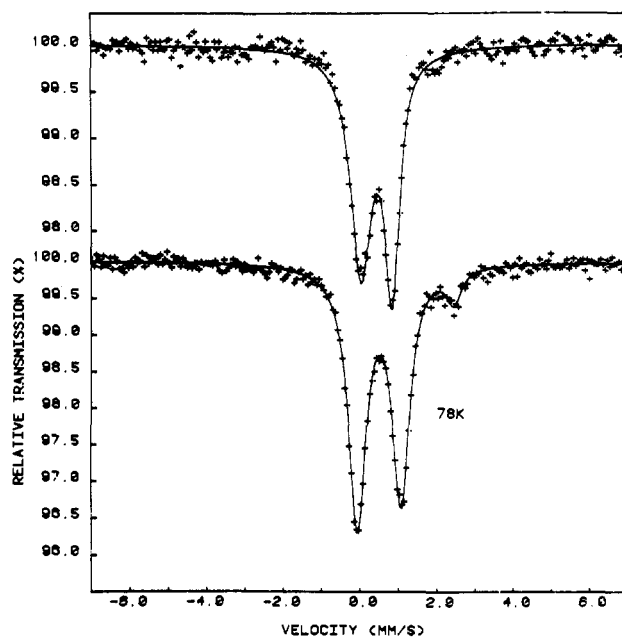


Figure 2. ^{57}Fe Mössbauer spectra of the intercalation compound $\text{FeOCl}((\text{CH}_3)_3\text{Sn}[\text{N}(\text{CH}_3)_2]_2)_{1/8}$: upper trace, 298 K; lower trace, 78 K. The isomer shift scale is with respect to Fe(0) at 298 K.

butions can be identified in the spectrum. Above ~ 140 K the hopping rate becomes faster than the Mössbauer time scale, and at room temperature the ^{57}Fe Mössbauer spectrum reflects the average of the Fe(II) and Fe(III) Mössbauer transitions. Because the sign of the principal electric field gradient tensor is opposite for the Fe(II) and Fe(III) sites,¹⁶ the relaxation process results in an averaging in which the room-temperature quadrupole splitting is smaller than that of the majority iron doublet at liquid-nitrogen temperature. The amount of charge donated to the host lattice per iron atom has been calculated by using this model and is included in Table III.

The extent of charge transfer to the lattice in organic intercalates of FeOCl is almost invariably 10–13%.¹⁶ This is presumably due to the bulk electrochemical potential of the Fe species in the lattice. In a study²⁰ of the electrochemical intercalation of Me_2SO -solvated lithium ions, potential steps were observed at 0.11 and 0.13 electron/iron in a galvanostatic reduction curve.

The charge transfer of INP1 (6.1%) is abnormally low, and in conjunction with the overall C, H, N inventory, this result corresponds to roughly equal amounts of positively charged and neutral guest species being present. The organotin amine intercalates are all within the 10–13% range. In INA1 the amounts of charged and neutral guest species are approximately equal, but in INA2 the charge transfer corresponds to considerably more charged than neutral guest species. For INA4 the charge-transfer results suggest that the predominant guest species present is doubly charged.

Infrared Spectroscopy. Infrared spectroscopy is a useful technique in studying the guest species in intercalation compounds of FeOCl because (unlike TaS_2) much of the spectral range from 600 to 2000 cm^{-1} is unobscured by absorptions due to the host material. Intercalation of pyridine was shown to result, in part, in the formation of guest pyridinium species for TaS_2 ¹⁰ and FeOCl.¹² It was thought that the intercalation of P1 might proceed by an analogous mechanism.

The infrared spectra of 4-(CH_3)₃Sn-py (P1), 4-(CH_3)₃Sn-py-(CH_3)₃SnCl (P2), and FeOCl(P1)_{1/7.5} (INP1) are shown in Figure 3. There are no published assignments for P1 or P2. The proximity of ring and methyl-associated modes makes the assignments derived from related model compounds less than satisfactory. However, the spectrum of INP1 does show evidence for the presence of a pyridinium ligand. An infrared study¹² of

(19) Davies, A. G.; Milledge, H. J.; Puxley, D. C.; Smith, P. J. *J. Chem. Soc. A* 1970, 2862.

(20) Meyer, H.; Weiss, A. *Mater. Res. Bull.* 1978, 13, 913.

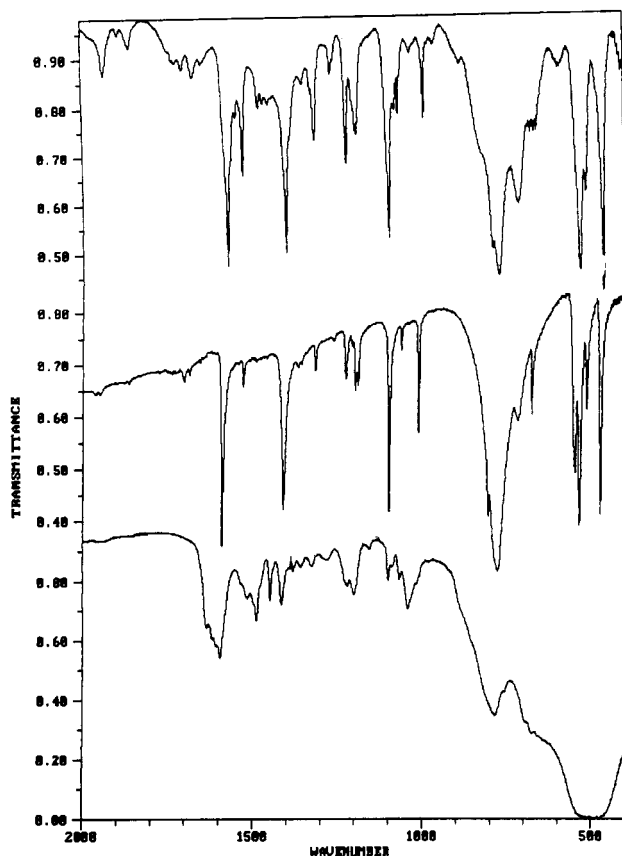
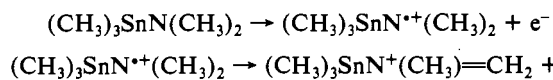


Figure 3. Transmittance infrared spectra (2000–400 cm^{-1}) of 4-(trimethylstannyl)pyridine (P1) (upper trace), 4-(trimethylstannyl)pyridine-trimethylstannyl chloride (P2) (middle trace), and the FeOCl intercalation compound with P1 (lower trace). The strong very broad absorption at $\sim 500 \text{ cm}^{-1}$ is due to the FeOCl matrix.

$\text{FeOCl}(\text{py})_{1/3}$ and $\text{FeOCl}(\text{py})_{1/4}$ and their perdeuterated analogues reported diagnostic bands for the presence of pyridine, pyridinium ion, and 4,4'-bipyridine. The two strongest diagnostic absorptions reported for the pyridinium ion—the 1191–1196- cm^{-1} in-plane C–H deformation and the 1634- cm^{-1} ring stretch—are both present in INP1 either as a new peak (1634 cm^{-1}) or as increased intensity of a peak present in the neat compounds [1204 cm^{-1} (vs, br)]. This supports the expected formation of a pyridinium species in INP1. The use of P2 as a model compound for the interpretation of the spectrum of INP1 will become evident in the next section.

The intercalation of ammonia in TaS_2 ²¹ was shown to result in the formation of guest ammonium ions. It was assumed that the intercalation of the organotin amines would proceed by an analogous mechanism, but the infrared data for the organotin amine intercalates could not be interpreted in terms of a substituted ammonium ion. A likely mechanism for the formation of a positively charged species is



This mechanism is similar to one of the two proposed by Audeh and Lindsay-Smith²² in which an iminium species is an intermediate in the oxidation of tertiary alkyl amines with potassium hexacyanoferrate(III).

To confirm this mechanism, the model intercalation compound $\text{FeOCl}[(\text{CH}_3)_2\text{N}^+=\text{CH}_2]_{1/5}[\text{Cl}^-]_{1/10}$ (INIM) was prepared. The C=N stretch that occurs in the neat iminium salt (also called a Schiff base), $(\text{CH}_3)_2\text{N}^+=\text{CH}_2\text{Cl}^-$, near 1672 cm^{-1} is observed in INIM at 1694 cm^{-1} . This region of the neat organotin amine

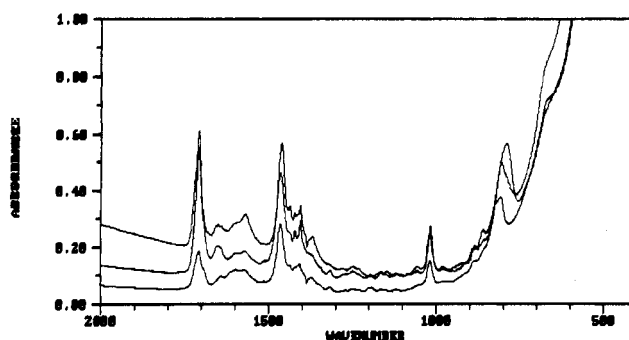


Figure 4. Absorbance infrared spectra (2000–400 cm^{-1}) of the three organotin amine intercalation compounds of FeOCl discussed in the text: upper trace, $\text{FeOCl}[(\text{CH}_3)_3\text{SnN}(\text{CH}_3)_2]_{1/3.5}$ (INA1); middle trace, $\text{FeOCl}[(\text{CH}_3)_2\text{Sn}[\text{N}(\text{CH}_3)_2]_{2/1.8}]_{1/8}$ (INA2); lower trace, $\text{FeOCl}[(\text{CH}_3)_2\text{N}]_4\text{Sn}_{1/16}$ (INA4).

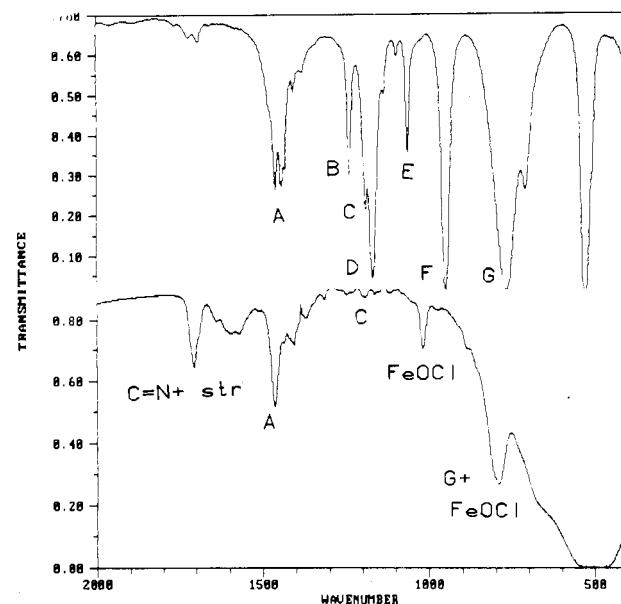


Figure 5. Transmittance infrared spectra (2000–400 cm^{-1}) of (tri-methylstannyl)dimethylamine [A1] (top trace) and its intercalation compound with FeOCl (lower trace). Key: A = CH asymmetric stretch; B = N methyl rock; C = CH bend; D = CNC asymmetric stretch, methyl rock; E = N methyl rock; F = N methyl rock, CNC asymmetric stretch; G = tin methyl rock.

spectrum is relatively transparent. All three organotin amine intercalates have strong absorptions at 1706–1707 cm^{-1} , indicating that iminium moieties are formed. The absorptions in this region are not due to the FeOCl lattice, since the spectrum of INP1 is also transparent in this region.

The infrared spectra of these neat organotins are very similar, the only major difference being the (tin) methyl rocking mode near 765 cm^{-1} in A1 and A2 that is absent, as expected, in A4. The infrared spectra for the corresponding three intercalates are also very similar. The absorbance infrared spectra of these three intercalates are shown in Figure 4. Except for intensity differences—as expected in a homologous series—the spectra are nearly identical except for the region near 800 cm^{-1} , where some shifting of the peak location is observed (vide infra).

The transmittance infrared spectra of A1 and INA1, shown in Figure 5, are now discussed in more detail. The assignments for A1 have been given by Marchand et al.²³ Only one assignment reported by Marchand et al. is questioned. These workers listed 1458 cm^{-1} (m) as a (N)–C–H asymmetric bend and 1435 cm^{-1} (m) as a (Sn)–C–H asymmetric bend. However in A4, where there are no tin–methyl bonds, Bürger and Sawodny²⁴ list 1460

(21) Schöllhorn, R.; Zagefka, H. D. *Angew. Chem.* **1977**, *89*, 193; *Angew. Chem., Int. Ed. Engl.* **1977**, *16*, 199.

(22) Audeh, C. A.; Lindsay-Smith, J. R. *J. Chem. Soc. B* **1970**, 1280.

(23) Marchand, A.; Forel, M.-T.; Riviere-Baudet, M.-H. *J. Organomet. Chem.* **1978**, *156*, 341.

Table IV. ^{119}mSn Mössbauer Data for 4-(Trimethylstannyl)pyridine (P1), 4-(Trimethylstannyl)pyridine-Trimethylstannyl Chloride (P2), and the Intercalation Compound Formed from FeOCl and 4-(Trimethylstannyl)pyridine (INP1)^a

	P1	P2		INP1	
		inner	outer	inner	outer
IS(78 K), mm s ⁻¹	1.29	1.29	1.36	1.29	1.42
QS(78 K), mm s ⁻¹	0.61	0.86	3.39	0.71	3.38
-d(ln A)/dT × 10 ²	3.40	2.70	2.22	2.08	1.85
MB area ratio ^b		0.98	1.00	0.81	1.00
⁵⁷ Fe MB neutral: charged ratio				1.00	0.81

^aReported values are typically ± 0.02 mm s⁻¹. ^bExtrapolated to 0 K.

(s) and 1430 cm⁻¹ (m) as (N)-C-H asymmetric bending modes. This suggests that the differentiation of nitrogen-bonded and tin-bonded C-H bending modes, as assigned by Marchand et al.,²³ may not be valid. The other assignments listed in Figure 5 are those of Marchand et al.²³ and are separated into vibrations associated with the tin-methyl group, the amino-methyl group, or both. Comparison of the spectral intensities of the neat compound with those of the intercalate shows with striking clarity the power of Fourier transform infrared spectroscopy in studying the interaction of the guest species within the host lattice. The four intense amino-methyl-associated vibrations in the neat compound are absent or, at best, weak in the spectra of the intercalate. This behavior is expected if the amino groups are the entities that hold the lattice apart and if their vibrations are suppressed by the steric crowding of the lattice.

There are three modes originating only from the tin-bonded methyls. A (tin) methyl rocking mode at 710 cm⁻¹ in the neat compound is obscured by an intense broad lattice absorption. The (tin) methyl rocking mode at 768 cm⁻¹ (vs, br) in the neat compound lies near a medium-intensity absorption at 813 cm⁻¹ in unintercalated FeOCl. The absorption at 790 cm⁻¹ (s, br) in the intercalate is presumably the resultant of these two absorptions. In INA4, where there are no tin methyl groups, this peak occurs at 809 cm⁻¹ (s, br). The fact that the resultant intercalate absorption is strongly shifted among the three organotin amine intercalation compounds suggests that this vibration is not significantly suppressed. Finally, the last tin-associated mode at 1190 cm⁻¹ in A1 is also present as weak absorption in the intercalate at 1192 cm⁻¹. These results suggest that, in contrast to the amine-associated modes, the tin-associated modes are not suppressed and therefore are not sterically affected by guest-guest or guest-host crowding. Moreover, the spectral region assigned to C-H bending evidences absorptions that apparently have contributions from both tin-methyl- and amine-associated modes and are intense in both the neat compound and the intercalation compounds. The intensity in the intercalation compound is presumably due to the tin-methyl-associated modes only.

^{119}mSn Mössbauer Spectroscopy. ^{119}mSn Mössbauer spectroscopy is an equally powerful technique for the study of these organotin intercalation compounds. The ^{119}mSn Mössbauer data presented here either suggest an unexpected structure for the guest species (in the case of INP1) or substantiate the structures previously advanced (the organotin-amine intercalates).

The 78 K ^{119}mSn Mössbauer spectra of 4-(trimethylstannyl)pyridine (P1), 4-(trimethylstannyl)pyridine-trimethylstannyl chloride (P2), and INP1 are shown in Figure 6. The pertinent ^{119}mSn Mössbauer data are listed in Table IV. The Mössbauer data for P1 and P2 have been discussed earlier.¹⁴ The ^{119}mSn Mössbauer spectrum of P1 shows an unresolved quadrupole split doublet. P2 was obtained as a byproduct in the synthesis of P1 and was determined to be an association compound of P1 with trimethylstannyl chloride. The spectrum of P2 is interpreted in terms of a four-coordinate tetrahedral tin site (inner doublet) and a five-coordinate trigonal-bipyramidal tin site (outer doublet) with the methyl groups occupying the equatorial positions. The large

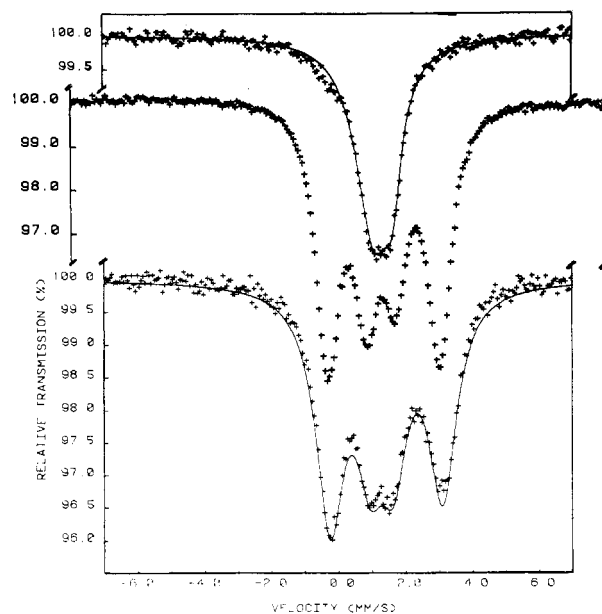


Figure 6. ^{119}mSn Mössbauer spectra at 78 K: upper trace, 4-(trimethylstannyl)pyridine (P1); middle trace, 4-(trimethylstannyl)pyridine-trimethylstannyl chloride (P2); bottom trace, FeOCl intercalation compound formed with P1. The isomer shift scale is with respect to BaSnO_3 at 295 K. In the lower trace, the solid line represents the fit to the experimental data using the parameters listed in Table IV (see text). The interpretation of the Mössbauer resonance spectrum for P2 has been discussed in ref 14.

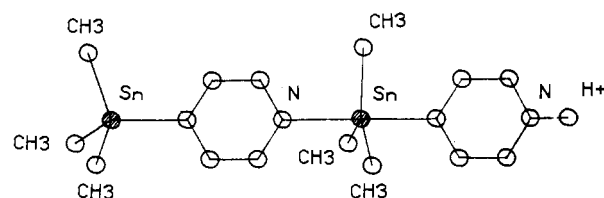


Figure 7. Proposed intercalated species for the FeOCl intercalation compound formed with 4-(trimethylstannyl)pyridine (INP1).

quadrupole splitting of the five-coordinate site is typical of a trigonal-bipyramidal ligand configuration around the metal atom.

The nearly identical Mössbauer parameters for P2 and INP1, including the relative areas under the two sets of quadrupole doublet resonances, indicate that four- and five-coordinate tin sites (in nearly equal populations) are present in the intercalate. The proposed structure of the guest species in INP1 is shown in Figure 7. The pyridinium ligand, which was suggested as the charge-carrying moiety by infrared spectroscopy, is attached to the five-coordinate tin site. Formation of the 4-(trimethylstannyl)pyridinium ion from 4-(trimethylstannyl)pyridine should open up the methyl-tin-methyl bond angles according to Bent's rule,²⁵ which postulates that when a metal atom is bonded simultaneously to two ligands of differing electron withdrawing power, p density will concentrate in the bond to the more electronegative ligand, whereas the metal orbital directed toward the more electropositive ligand will be enriched in s character. Since the methyl-tin bonds have enhanced s character after the pyridinium ligand is formed, the methyl-tin-methyl bond angles increase, facilitating the attack of another 4-(trimethylstannyl)pyridine to form the associated complex.

The proposed guest species accounts for the unexplained results in the X-ray powder diffraction and ^{57}Fe Mössbauer studies. The interlayer expansion in INP1 was shown to be too large to be due to a tetrahedral trimethylstannyl or pyridine group holding apart the FeOCl layers. For the proposed guest species the upright planar trimethylstannyl group is suggested as the moiety that

(24) Bürger, H.; Sawodny, W. *Spectrochim. Acta, Part A* 1967, 23A, 2841.

(25) Bent, H. A. *J. Chem. Educ.* 1960, 37, 616; *J. Chem. Phys.* 1960, 33, 1258; *Chem. Rev.* 1961, 61, 275.

Table V. ^{119}mSn Mössbauer Parameters for the Neat Organotin Amines and Their Corresponding Intercalation Compounds in FeOCl^a

	A1	A2	A4			
IS(78 K), mm s ⁻¹	1.235	1.163	0.846			
QS(78 K), mm s ⁻¹	0.917	1.222	0			
-d(ln A)/dT × 10 ²	2.85	2.14	1.95			
	INA1 ^{b,c}		INA2 ^c		INA4	
	inner neut	outer chgd	inner neut	outer chgd	dbly chgd	
IS(78 K), mm s ⁻¹	1.124	1.412	1.691	1.276	0.138	
QS(78 K), mm s ⁻¹	2.608	3.182	<1	2.844	0.658	
-d(ln A)/dT × 10 ²	1.10	1.61	0.67	1.26	0.66	
tin MB area ratio ^e	0.67	1.0	0.04	1.00	1.00	0
iron MB charged: neutral ratio	1.00	0.78	0.22	1.00	1.00 ^d	0.14

^a Reported values are typically ± 0.03 mm s⁻¹. ^b 80 K. ^c Mössbauer line widths fixed in fitting procedure. ^d Doubly charged:neutral ratio. ^e Extrapolated to 0 K.

actually determines the interlayer spacing. The abnormally low charge transfer to the lattice, as determined by ^{57}Fe Mössbauer spectroscopy, can also be accounted for by the proposed species. Comparison of the neat guest molecular dimensions with the lattice space available according to the stoichiometry indicates that the guest species forms a "full" monolayer between each FeOCl layer. The proposed species is consistent with the following results: (1) The extent of charge transfer to the lattice: the stoichiometry (with the proposed species) predicts 6.7% compared with 6.1% calculated from the ^{57}Fe Mössbauer results. The abnormally low charge transfer to the lattice in INP1 is therefore due to the large size of the singly charged guest species. Parenthetically, the calculated results underestimate the true charge transfer in this compound because the ^{57}Fe spectrum normally used as representing the slow exchange limit, the 78 K spectrum, showed considerable antiferromagnetic ordering, and the 100 K spectral data were used instead. (2) The near equality of the population of "charged" and "uncharged" tin moieties in the lattice as determined by ^{57}Fe relaxation calculations and by ^{119}mSn Mössbauer areas: the ^{119}mSn Mössbauer area ratios underestimate the "uncharged" tin moieties because the recoil-free fraction at 0 K for the tetrahedral tin site does not equal that for the trigonal-bipyramidal site. This is unusual, but would be expected for a tin species in an occupied-cage type structure where the tin species has room to execute large amplitudes of vibration, even in the low-temperature limit.

The ^{119}mSn Mössbauer data of the three neat organotin amines and their corresponding intercalates are listed in Table V. In addition, the spectra are shown in Figure 8. The spectrum of A4 is a narrow line singlet while the spectra of A1 and A2 show quadrupole split doublets. The observed isomer shifts are all characteristic of organotin(IV) compounds. The substantial changes in the quadrupole splitting parameter on intercalation are indicative of a major change in the charge distribution around the metal atom. INA4 is a broad singlet, indicative of an unresolved quadrupole hyperfine interaction. The remaining spectra are more readily interpreted along with the results from the charge-transfer calculations and the observed stoichiometries. INA1 and INA2 are expected to have at least two different tin environments, corresponding to "charged" and "neutral" tin moieties. In INA1 these should be present in a roughly 1:1 ratio. The spectrum of INA1 shows one narrow and one broad absorption of unequal intensity but roughly equal area. The only assignment of these peaks consistent with reasonable Sn(IV) isomer shifts is for the presence of two quadrupole split tin sites, where the more negative velocity components are of nearly equal energy, with somewhat different energies for the more positive velocity components. For INA2, the more abundant charged guest species is manifested by the majority quadrupole split doublet. The less abundant neutral species is represented by a weak shoulder (presumably a broad singlet) on the more positive majority velocity peak.

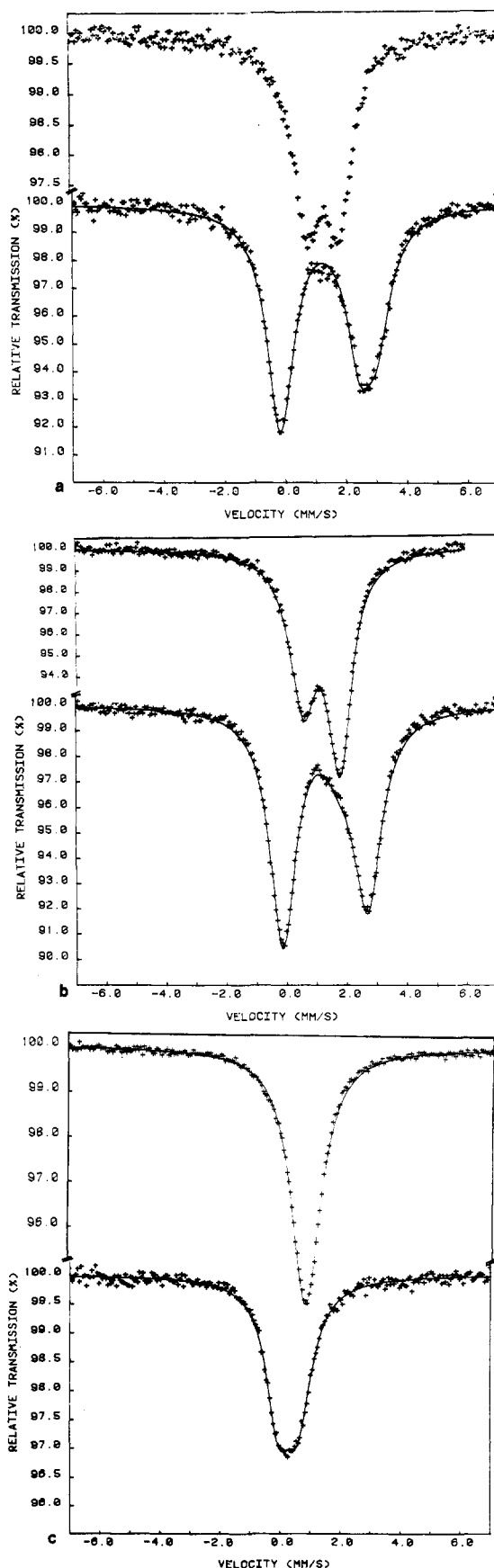


Figure 8. ^{119}mSn Mössbauer spectra at 78 K of the neat organotin compounds (upper trace) and their FeOCl intercalation compounds (lower trace) discussed in the text: (a) (dimethylamino)trimethylstannane; (b) bis(dimethylamino)dimethylstannane; (c) tetrakis(dimethylamino)stannane. In each case the isomer shift scale is with respect to BaSnO_3 at 295 K. The solid curves represent the fit to the data using the parameters listed in Table V.

The isomer shifts of the neat organotin amines show the expected decrease across the series from A1 to A4. The isomer shift reflects the tin *s* electron density at the nucleus. For ^{119m}Sn the isomer shift decreases when the electron density is drained from the tin bonding orbitals that have at least partial *s* character. In the present instance the electronegative dimethylamino ligand withdraws more electron density from the tin orbitals than the methyl ligand. In comparing the isomer shifts of the neat organotin amines with the corresponding intercalates, there are two predominant effects to be considered. First, the isomer shift in neutral six-coordinated tin compounds²⁶ is generally larger than that expected for the neat four-coordinate analogues. Second, the isomer shift is expected to decrease when a neutral amino ligand is replaced with a charged iminium ligand. The isomer shift of neutral INA2 reflects the increase of the isomer shift in going to six-coordination. The isomer shift of neutral INA1 is abnormally low and is not understood but was assigned on the basis of the stoichiometry of an independent sample, in which the ratio of neutral to charged metal centers was approximately 0.4, leading to a readily identifiable asymmetry in the Mössbauer spectrum. The IS of charged INA2 is higher than that of the neutral compound (due to the increase in coordination) but lower than neutral INA2 (charged ligand effect). The IS of charged INA1 is in line with expectations, i.e. slightly larger than that of A1 and slightly larger than that of charged INA2. The INA4 isomer shift is very low, reflecting the fact that these guest species are doubly charged.

The $-\text{d}(\ln A)/\text{d}T$ values measure the change in recoil-free fraction with temperature. A "stiff" lattice, i.e. as observed in most inorganic tin compounds that are ionically bonded, has low $-\text{d}(\ln A)/\text{d}T$ values. Organometallic tin compounds, in which the intermolecular bonding is weak, have high $-\text{d}(\ln A)/\text{d}T$ values.²⁷ The numerical value of the recoil-free fraction reflects the mean-square amplitude of vibration of the Mössbauer probe atom and can be related to a number of factors, including the nature of the ligands bonded to the tin atom, as well as the strength of the inter- and intramolecular forces affecting the motion of this atom. The decrease in the absolute magnitude of $-\text{d}(\ln A)/\text{d}T$ across the neat series is accounted for by the increase in ligand mass. This trend is not seen with the intercalate data. It was proposed that the amino ligand is holding the host layers apart and that the methyl groups (and to a lesser extent the iminium groups) are in free space. The presence of an amino ligand bonded to the tin should therefore increase the recoil-free fraction and

lower $|\text{d}(\ln A)/\text{d}T|$. The trend in $|\text{d}(\ln A)/\text{d}T|$ values for the guest species can now be accounted for, on the basis of the number of amino groups present in the species. There are two amino groups in doubly charged INA4 and neutral INA2, and these have the lowest values of $|\text{d}(\ln A)/\text{d}T|$. Charged INA1, which does not have amino groups (but where the lattice is still presumably held apart by the accompanying neutral species with amino groups), has the highest value of this parameter. Finally, neutral INA1 and charged INA2 each have one amino ligand and have intermediate $|\text{d}(\ln A)/\text{d}T|$ values.

Summary and Conclusions

The four organotin intercalation compounds reported here have been shown to form via the redox mechanism proposed by Schöllhorn. In the INP1 intercalate, the infrared results support the presence of a pyridinium ligand as the charge-carrying moiety. In addition, the abnormally low charge transfer to the lattice and ^{119m}Sn Mössbauer data can only be reasonably interpreted in terms of an associated binuclear tin compound containing four- and five-coordinate tin sites.

The three organotin amine compounds change from four-coordinated to six-coordinated tin upon intercalation. The infrared spectra of these compounds suggest that the charge-carrying ligand in these systems is an iminium species. Significant concentrations of accompanying neutral guest species in the INA1 and INA2 compounds, as calculated from elemental analysis and from the charge transfer (deduced from the ^{57}Fe Mössbauer results), are substantiated by the ^{119m}Sn Mössbauer spectroscopy results. The INA4 species, which was predicted to be predominantly present as the doubly charged species from the ^{57}Fe Mössbauer results, was also substantiated by the ^{119m}Sn isomer shift.

The infrared results for these three compounds also suggested that the amino group is the entity that holds the layers of FeOCl apart in the intercalation compound. This effect is also substantiated by the monotonic dependence of the ^{119m}Sn Mössbauer $|\text{d}(\ln A)/\text{d}T|$ values as a function of the number of amino groups present in the particular species.

Acknowledgment. This research was supported in part by Grant DMR 8102940 from the Division of Materials Research of the National Science Foundation and by a grant from the Center for Computer and Information Services of Rutgers University. The authors are also indebted to Dr. Hellmut Eckert for performing the charge-transfer calculations and for many helpful discussions.

Registry No. INP1, 102941-80-0; INA1, 102941-81-1; INA2, 102941-82-2; INA4, 102941-83-3; INIM, 102941-84-4.

Supplementary Material Available: Tables of X-ray powder diffraction data for FeOCl and the five intercalation compounds discussed in the text (6 pages). Ordering information is given on any current masthead page.

(26) Fitzsimmons, B. W.; Seeley, N. J.; Smith, A. W. *J. Chem. Soc. A* **1969**, 143.

(27) Zuckerman, J. J. In *Chemical Mossbauer Spectroscopy*; Herber, R. H., Ed.; Plenum: New York, 1984; Chapter XI; see also Chapter VII.